INTERNATIONAL ATOMIC ENERGY AGENCY
UNITED NATIONS EDUCATIONAL, SCIENTIFIC AND CULTURAL ORGANIZATION
INTERNATIONAL CENTRE FOR THEORETICAL PHYSICS
I.C.T.P., P.O. BOX 586, 34100 TRIESTE, ITALY, CABLE: CENTRATOM TRIESTE

H4.SMR/383 - 28

WORKSHOP ON REMOTE SENSING TECHNIQUES WITH APPLICATIONS TO AGRICULTURE, WATER AND WEATHER RESOURCES

(27 February - 21 March 1989)

RAINFALL ESTIMATION TECHNIQUES

INES VELASCO
Universidad de Buenos Aires
Departamento de Meteorologia
Pabellon Ii. 2 do Piso
Buenos Aires 1428
ARGENTINA

II. RAINFALL ESTIMATION TECHNIQUES

II.1 INTRODUCTION

Precipitation information is a primary requirement of hydrologists and agriculturalists around the world. Also of utmost importance is the need to estimate areas of heavy precipitation prior to inssuance of flash flood or winter storm warnings and special weather statements. Hydrologists, meteorologists and river forecasters use precipitation estimates as an aid in their evaluation or prediction of flood potential. Precipitation information is extremely useful for energy balance considerations in climatological studies.

Satellite-derived precipitation estimation techniques ranging in uses from the mesoscale to the climate scale are covered by Barrett and Martin (1981). Most schemes are variants of the basic idea that since it rains under clouds, if one knows where the clouds are, one knows where it is raining.

Techniques for estimating rainfall from satellites have typically used two types of measurements:

1) The use of visible (VIS) and infrared (IR) measurements is based on empirical relationships between cloud parameters and the resultant precipitation. Such cloud parameters include size, growth rates and cloud top temperatures.

2) The use of microwave measurements has been based on theoretical relationships between rain rates and the satellite-measured values. The basis for the microwave method is somewhat similar to that behind ground-based radar reflectance measurements and rainfall, but using passive radiometers. This chapter will only briefly cover these techniques.

II.2 VIS AND IR TECHNIQUES

There are two basic types of VIS and IR precipitation estimation techniques: cloud history and indexing. VIS and IR methodologies infer precipitation amounts for specific cloud features. Cloud history works best where geostationary satellite data are available. The frequent views from geostationary satellites allow the life cycle of a cloud to be followed and precipitation estimates to be computed for each stage of the cloud's development. In contrast, cloud indexing is the principal method used when only polar-orbiter satellite data are available; only two pictures a day can be obtained from a single polar-orbiting satellite. Cloud indexing involves characterizing a cloud by an index number according to its appearance in imagery and then using a look-up table or regression equation to estimate the precipitation from the cloud. Both the cloud history and cloud indexing methods have procedures for modifying the estimates for different climates and environments.

Estimates of rainfall are a function of the following:

- Dominant organization of the synoptic weather.
- Proportion of sky that is cloud covered.
- Intensity of rain, which is influenced by the types of cloud present, cloud top temperature/cloud growth, overshooting tops, mergers, etc.

The intended use of the precipitation analysis determines the size of the area over which the estimates are computed: small areas for heavy rain, large areas for climate.

Refinements on the techniques can be based on knowlewdge of the fractional cloud cover, cloud type, visible brightness, IR temperature and area or areal growth rates of clouds. The accuracy of such techniques improves with increasing averaging time and with increasing averaging area.

A statistical relationship between rainfall volume and cloud properties can be established.

$$R_v = \sum_{i=1}^{m} C_{0,i} + C_{1,i}A_i + C_{2,i}(dA_i/dt) \quad (1)$$

where

R_v = Rainfall volume over specified domain (x,y,z)

A_i = Areal coverage of cloud type i

$\frac{dA_i}{dt}$ = Growth or decay rate of cloud type i

$C_{i,i}$ = Empirical coefficients

Generally, $C_{0,i} = 0$. Only Barret (1973) and Folansbee (1973) have allowed $m \geq 1$. Few have set $C_{2,i} \neq 0$; this term is generally small.

A notable scheme includes Scofield and Oliver (1977) and Scofield (1987) in which estimates of point convective precipitation rates are based on visible and enhanced infrared GOES imagery. A decision tree process is used. The scheme "underestimates" the rainfall up to 30 % in extreme rainfall situation (≥ 50 mm·h^{-1}) and overestimates rainfall up to 30 % for light to heavy rainfalls (≤ 50 mm·h^{-1}). (For more details see II.6).

Griffith et al. (1976,1978) designed a system to measure precipitation over fairly large areas by considering the rainfall from each cloud using GOES visible or infrared data at 1/2 hour resolution. The scheme uses a two-step correlation between the area of the cloud and the expected area of the radar echo underneath the cloud. The area of the cloud is then related to the volumetric rain rate

$$R_v = I \cdot A_E \quad (2)$$

where

A_E = area of radar echo (km^2)

R_v = volumetric rain rate ($m^3 \cdot s^{-1}$)

I = intensity = 4.33 (echo area increasing)

= 3.27 (echo area constant)

= 2.20 (echo area decreasing)

Table II.1 lists many studies which have used visible and infrared iamgery to estimate precipitation from satellites. Such techniques have problems. A basic problem is the lack of a solid physical relationship between rainfall and cloud parameters.

Cheng and Rodennuls (1977) concluded that :thresnhold techniques may be used with only limited success in determining the intensity of precipitation. If this is correct, the success of quantitative precipitation estimates by remote sensing reported by other authors is due more to the time-integration of a reasonable rainfall rate rather than successfully estimating intense rainfall rates."

II.3 MICROWAVE TECHNIQUES

The primary advantage of microwave measurements is their ability to penetrate through clouds, rain being the major source of attenuation for the "window" frequencies below 50 GHz. Furthermore, over low-emissivity sea surfaces the brightness temperature measurements in clearer areas are highlighted against the more emissive, warmer measurements in precipitating regions. The large contrast (>50 K) in brightness temperature between the rain and its surroundings has stimulated much interest in applying microwave radiometry over oceans for determining rainfall. The global distribution of rainfall over the oceans was also attempted from satellite measurements (Rao et al.,1976).

II.4 SINGLE-FREQUENCY TECHNIQUE

In most situations it is sufficient to relate rain intensity directly to increase in brightness temperature over oceans. Effects such as those of sea surface winds on emissivity or the contributions due to cloud and water vapor absorption are of second order and can usually be neglected.

The more variable and higher emissivity of land presents problems because of the similarity in brightness temperature of rain and land. Also, decreases in surface emissivity due to wet ground and snow cover can produce false precipitation signatures if not accounted for (Rodgers and Sidalingaiah, 1983). Only in the case of heavy thunderstorms can the rain measurements be much lower (>50 K) than the surrounding brightness temperatures. The enhacement for the intense storms is principally due to the scattering of upwelling radiation by large ice particles at the tops of rain layers. This scattering effect increases with increasing frequency, and was first noted during observation of convective storms over the United States, using scanning multichannel microwave radiometers (SMMRs) (Spencer et al., 1983). Brightness temperatures as low as 163 K were obtained at the center of an intense storm for the highest frequency (37 GHz) channel.

In the case of stratiform rain the contribution due to scattering is small. To identify rain one must use the smaller difference between the thermal emission from precipitation drops and that from the land background. Dual frequency and/or polarization techniques are being developed to enhance the precipitation signature over land by minimizing the effect of surface emisivity on the microwave measurements. These approaches use statistical correlations between emissivities at different frequencies of between the two polarizations.

II.5 FREQUENCY SCREENING

For many surfaces the emissivity has either very little frequency dependence or increases with frequency. This is a true for wet and dry soil, vegetation, open water, melting snow, lake ice, and new sea ice. In contrast, brightness temperatures of rain cells decrease with increasing frequency; i.e., temperatures are due to scattering and thermal emission. It is therefore possible to isolate the precipitation signature by measuring the difference between the brightness temperatures at two frequencies $-T_b(\nu_1) - T_b(\nu_2)$, where $\nu_2 > \nu_1$ and displaying only the positive values. However, surfaces such as dry snow have a frequency response similar to that of rain, and would not be screened out. This problem can be alleviated by viewing sequential measurements and associating the rapid changes with precipitation. Also, the brightness temperature sum at the two frequencies $[\ T_b(\nu_1) + T_b(\nu_2)\ ]$ can be used to make the final discrimination (i.e., stratiform rain has higher brightness temperatures than dry snow).

Separating snow cover from rainfall requires the use of the brightness temperature sum as well as the difference. For example, the cluster diagram of Fig. II.1 is based on the January measurements from the Gulf of Mexico to Hudson Bay, The clusters corresponding to dry snow and to rain both lie in the positive quadrant. Fortunately, they are separated vertically by brightness temperature. The negative quadrant contains clusters formed by dry soil, wet land along the Mississippi Delta, and open water in the Great Lakes and Gulf of Mexico. The scattered points between the wet land and open water correspond to fields of view containing mixtures of different surfaces, e.g. land and water. The small cluster labeled lake ice represents data from over Hudson Bay.

Frequency screening uses the correlation between emissivities at different frequencies to enhance the precipitation signature.

II.6 HEAVY PRECIPITATION AND FLASH FLOOD FORECASTING

VIS and IR data are being used operationally for analyzing and forecasting heavy precipitation events. Satellite-derived precipitation estimates and 3 h precipitation trends for convective systems (Scofield and Oliver, 1977; Scofield, 1987; and Spayd and Scofield, 1984a), extratropical cyclones (Scofield and Spayd, 1984a), and tropical cyclones (Spayd an Scofield, 1984,b) are computed on the NESDIS Interactive Flash Flood Analyzer (IFFA) and transmitted to NWS Forecast offices, and River Forecast centers.

The operational NESDIS Convective Storm Technique gives half-hourly or hourly rainfall estimates for convective systems by using GOES IR and high-resolution VIS images. The technique is designed for deep convective systems that occur in tropical air masses with high tropopauses, and it uses IR images (Fig. II.2) digitally enhanced according to the Mb Curve (Fig. II.3) designed to help estimate convective storm intensity. Estimates of convective rainfall are computed by comparing changes in cloud character between two consecutive images. The technique is divided into three main steps (Fig. II.4).

The Convective Storm Technique has been modified so that the temperature of the convection computed from a sounding is compared with the observed cloud-top temeperature. This computed temperature (called the Equilibrium Level) (Fig. II.5) is the best measure of the expected anvil temperature and should be used for examining the anvil growth rates. Cloud top temperatures equal to or colder than the computer temperature would indicate heavier rainfall rates than warmer ones.

Accurate verification of operationally produced rainfall estimates for deep convective rainfall events is very difficult because of the extreme variations in the temporal and spatial distribution of convective precipitation. Studies of thunderstorm events over dense raingauge networks have shown that variations of up to 2 inches of rainfall over 1 n mi range in a half-hour period to occur.

Nevertheless, a verification study of the operationally produced rainfall estimates from May through July 1984 was completed by comparing the total maximum rainfall estimates for a storm (usually a period of 1 to 6 h) with the 24-hourly cooperative rainfall reports available the next day. Events that included less than two or three rainfall reports per county, and events in which additional rain fell outside the time rainfall estimates were produced, were eliminated; 268 events remained.

The verification results showed that the average error of the rainfall estimates for a storm total precipitation event is about 30 % . The absolute and average errors both increase as the magnitude of the event increases. For relatively small events (3.9 inches or less) there is a tendency to overestimate the event, and as the magnitude of the event increases there is a distinct tendency to underestimate. If a rainfall estimate is 4 inches or more, there is an excellent probability that at least 4 inches will be observed. Improved heavy precipitation estimates are possible when passive microwave data are combined with VIS and IR data.

Table II.1 CLASSIFICATION (AND ASSOCIATED AUTHORS) OF VISIBLE AND INFRARED BASED SATELLITE PRECIPITATION ESTIMATION METHODS.

Method	Authors
1.Direct Correlation	Lethbridge (1967) Gerrisch (1970) Kilonsky and Ramage(1976) (Cheng and Rodenhuils (1977a,1977b) (Silva Dias et al. (1977)
2.Nephanalysis	Barrett (1970,1973) Follansbee (1973,1975,1976)
3.Radar Analog	
a. Empirical	Sherer and Hudlow (1971) Sorman (1972)
b. Parameterization	Gruber (1973)
4.Mass Transport/Radar Analog	Griffith and Woodley (sequence or reports and publications from 1971 to 1979). Martin, Sikdar and Stout (sequence of reports and publications from 1975 to 1979).
5.Hydrological Interence	Rainbird (1969) Grosch and Weinman (1973)
6.Decision Tree	Scofield and Oliver (1977) Adler and Fenn (1976,1977,1978) Reynolds and Smith (1979) Schultz and Klatt (1980) Scofield (1984)

CHAPTER II.

REFERENCES AND SUPPLEMENTARY READING

Barret, E.C., 1973. Forecasting daily rainfall from satellite data. Mon. Wea. Rev., 98, 322-327.

Barret, E.C.,and D.W. Martin, 1981. The Use of Satellite Data in Rainfall Monitoring, Academic Press, New York, 340 pp.

Cheng, N. and D. Rodenhuils, 1977. An intercomparison of satellite images and radar rainfall rates. Postprints, 11th Technical Conference on Hurricanes and Tropical Meteorology, AMS, Boston, MA, 224-226.

Clark, J. Dane, 1983. The GOES User's Guide. Office of Satellite Data Processing and Distribution.

Follansbee, W.A., 1973. Estimation of average daily rainfall from satellite cloud photographs. NOAA Tech. Memo. NESS-44, U.S. Dept. of Commerce, Washington, DC, 39 pp.

Fleming, E.L. and L.E. Spayd, Jr.. 1986. Characteristics of western region flash flood events in goes imagery and conventional data. NOAA Tech. Memo. NESDIS 13, Satellite Applications Laboratory, Washington, D.C., 82 pp.

Griffith, C.G., W.L. Woodley, S. Browner, J. Teijeiro, M.Maler, D.W. Martin, J.Stout and D.N. Sikdar, 1976. Rainfall estimation from geosynchronous satellite iamgery during daylight hours. NOAA Tech Report ERL 356-WMPO 7, U.S. Dept. of Commerce, Boulder, CO, 106 pp.

Griffith, C.G., J.A. Augustine, W.L. Woodley, P.G. Grube, D.W. Martin, J. Stout and D. N. Sidkar, 1978. Rain estimation from geosynchronous satellite imagery - visible infrared studies. Mon. Wea. Rev., 106, 1153-1171.

Rao, M.S.V., W.V. Abbott, III, and J.S. Theon, 1976. Satellite-derived global oceanic rainfall atlas (1973 and 1974) NASA SP-410, Washington, D.C. (NTIS#N77-19709).

Rockwood, A.A., D.L. Bartels and R.A. Maddox. 1984. Precipitation characteristics of a dual mesoscale convective complex. NOAA Tech. Memo. ERL ESG-6, Environmental Sciences Group, Boulder, Colorado, 50pp.

Scofield, R.A., and V.J. Oliver,1977; A scheme for estimating convective rainfall from satellite imagery. NOAA Tech. Memo. NESS-86, National Earth Satellite Service, Washington, D.C. (NTIS-#PB-270762/8G1), 47 pp.

Scofield, R.A., 1984; The NESDIS operational convective precipitation estimation technique. Preprints, 10th Conference on Weather Forecasting and Analysis, Clear-

water Beach, American Meteorological Society, Boston, 171-180.

Scofield, R.A. and L.E. Spayd, Jr., 1984; A technique that uses satellite, radar and conventional data for analyzing and short-range forecasting of precipitation from extratropical cyclones, NOAA Tech. Memo. NESDIS-8, National Environmental Satellite, Data and Information Service, Washington, D.C. (NTIS#PB85-164994), 51 pp.

Shi, J. and R.A. Scofield. 1987. Satellite observed mesoscales convective system (MCS) propagation characteristics and a 3-12 hour heavy precipitation forecast index. NOAA Tech. Memo NESDIS 20, Washington, D.C., 43 pp.

Spayd, L.E., Jr., and R.A. Scofield , 1984a: An experimental satellite-derived heavy convective rainfall short range forecasting technique. Preprints, 10th. Conference on Weather Forecasting abd Analysis, Clearwater Beach, American Meteorological Society, Boston, 400-408.

Spayd, L.E., Jr., and R.S. Scofield, 1984b: A tropical cyclone precipitation estimation technique using geostationary satellite data. NOAA Tech. Memo. NESDIS-5, National Environmental Satellite, Data an Information Service, Washington, D.C. (NTIS-#PB84-226703), 36 pp.

Spencer, R.W., W.S. Olson, Wu Rongshang, D. Martin, J.A. Weinman, and D.A. Santek, 1983; Heavy thunderstorms observed over land by the Nimbus-7 scanning multichannel microwave radiometer. J. Clim. Appl. Meteor., 22, 1041-1046.

VonderHaar, T.H., 1969. Meteorological applications of reflected radiance measurements from ATS 1 and ATS 3. J. Geophys. Res. 74:5404-5412.

Weinreb, M.P., and D.S. Crosby, 1973. Estimation of atmospheric profiles from satellite measurements by a combination of linear and nonlinear methods. Preprints, Third Conference on Probability and Statistics in Atmospheric Science, Boulder, Colorado. American Meteorological Society, Boston, Mass., 231-235.

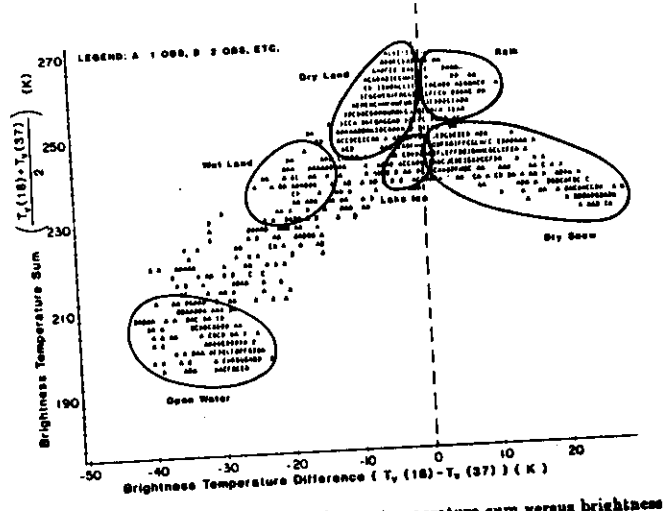

Figure II.1 Typical cluster diagram of brightness temperature sum versus brightness temperature difference; 18 and 37 MHz measurements were used. (From Scofield and Purdom, 1986).

ENHANCEMENT MB ✓

GENERAL DESCRIPTION

Segments 1, 2, and 3 are extracted directly from the old Z curve: This steeper slope will give better definition to the low and mid clouds. Segments 4 through 7 contours convective areas. Segment 8 slopes with a factor greater than zero from -63° C to -80° C which allows for good definitions of very cold domes. Although specific temperatures cannot be obtained--it better isolates the coldest tops by gradually going to white rather than producing a complete white-out at all temperatures colder than -65° C. This curve is utilized for rainfall estimates.

Fig. II.2 (From the GOES User's Guide, 1893)

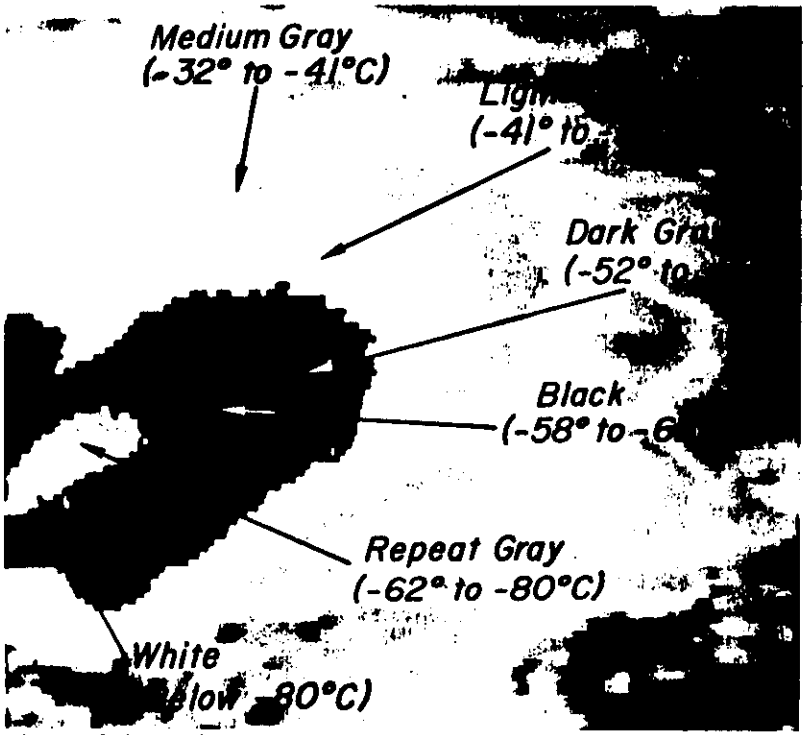

Fig. II.2 (From the GOES

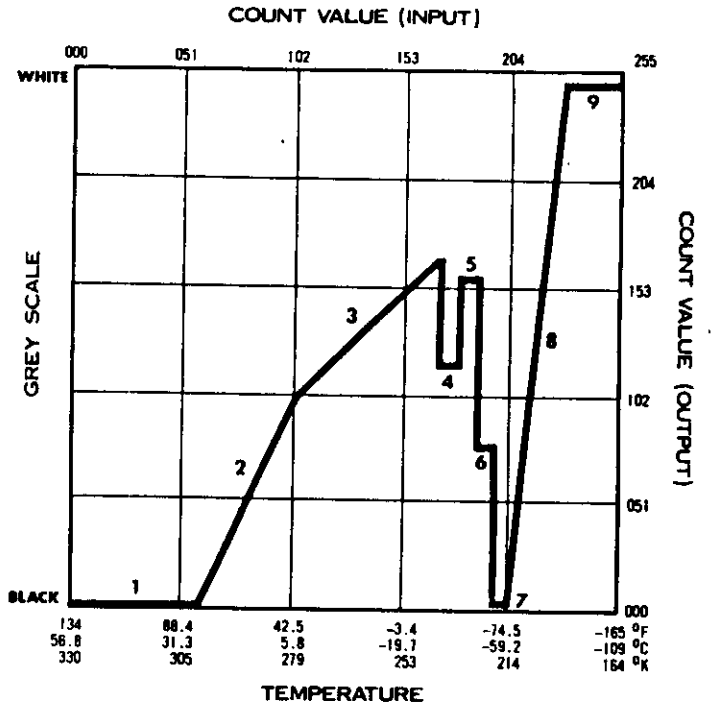

SEGMENT NUMBER	°C TEMPERATURE	COMMENTS
1	58.8 to 29.3	Little or no useful Met Data (Black)
2	28.8 to 6.8	Low Level/Sea Surface Difference
3	6.3 to -31.2	Middle Level - No Enhancement
4	-32.2 to -42.2	First Level Contour (Med Gray)
5	-43.2 to -53.2	(Light Gray)
6	-54.2 to -59.2	Thunderstorm (Dark Gray)
7	-60.2 to -63.2	Enhancement (Black)
8	-64.2 to -80.2	Overshooting Tops Enhancement
9	-81.2 to -110.2	(White)

FIG. II.3 (From the GOES User's Guide, 1983).

CONVECTIVE STORM TECHNIQUE

STEP 1

RAINFALL IS COMPUTED ONLY FOR THE ACTIVE PORTION OF THE THUNDERSTORM SYSTEM:

The following are clues for helping to make this decision.

- Area of IR temperature gradient at upwind end of anvil for a thunderstorm system in strong vertical wind shear.
- Center of the anvil with a tight, uniform IR temperature gradient around entire anvil for a thunderstorm system with no vertical wind shear.
- Area near and under an overshooting top.
- Portion of anvil that is brighter and/or more textured.
- Half of anvil bounded by edge which moves least (comparison of last two IR or VIS pictures).
- Area near "upper level" (500 - 200 mb) upwind end of anvil.
- Area near low-level inflow.
- Area under a radar echo.

STEP 2

HALF-HOURLY RAINFALL ESTIMATES IN MILLIMETERS ARE COMPUTED FROM THE FOLLOWING FACTORS:

FACTOR 1

CLOUD-TOP TEMPERATURE AND CLOUD GROWTH FACTOR.
Determine amount that the coldest cloud tops increased within half-hour and select estimate amount according to gray shade:

(Degrees in Centigrade)	>2/3° LAT	>1/3° <2/3° LAT	≤1/3° LAT or same	areal decrease of shade or warming from white to rpt gray or within the rpt gray	Coldest tops 1 or more shades warmer
Med Gray (-32 to -41°)	6	4	2	1	T
Lt Gray (-41 to -52°)	13	8	4	2	↓
Dk Gray (-52 to -58°)	19	10	5	4	
Black (-58 to -62°)	25	15	8	5	
Rpt Gray*(-62 to -80°)	25-50	15-25	8-15	8	↓
(EQUILIBRIUM LEVEL) White (below -80°)	50	25	15	10	2

*Colder repeat gray shades should be given higher rainfall estimates.

OR

DIVERGENCE ALOFT FACTOR.*
Determine estimate according to gray shade when strong divergence is apparent:

(EQUILIBRIUM LEVEL)					
Med Gray	Lt Gray	Dk Gray	Black	Rpt Gray	White
4	8	10	15	15-25	25

*IR imagery shows edges of thunderstorm anvil along the upwind end forming a large angle of between 50-90 degrees pointing into the 200 mb wind; 200-mb analysis often shows these storms just downwind from where the polar jet and subtropical jet separate.

GO TO FACTOR 2

Fig. II, 4 Step 1 and step 2 (factor 1) of the convective storm technique. (From Scofield 1987)

FROM FACTOR 1

FACTOR 2

OVERSHOOTING TOP FACTOR.* Estimate an additional 8 mm for colder tops in the area of the overshooting tops.

*High-resolution visible imagery is the best data for determining this factor.

FACTOR 3

THUNDERSTORM OR CONVECTIVE CLOUD LINE MERGER FACTOR. Estimate an additional 12.7 mm for colder tops in the area of the merger.

FACTOR 4

SATURATED ENVIRONMENT FACTOR. Estimate additional amount according to gray shade and time of persistence:

	(EQUILIBRIUM LEVEL)					
	Med Gray	Lt Gray	Dk Gray	Black	Rpt Gray	White
≥1 Hour but <2 Hours	5	5	5	5	8	8
≥2 Hours	10	10	10	10	13	13

FACTOR 5

MOISTURE CORRECTION FACTOR = Calculate factor as the product of the Precipitable Water (SFC-500MB) ° Relative Humidity (SFC -500 MB)

STEP 3

FACTORS 1 THROUGH 4 ARE SUMMED AND MULTIPLIED BY MOISTURE CORRECTION FACTOR:

TOTAL HALF-HOURLY CONVECTIVE RAINFALL ESTIMATES (in millimeters) =

[(Cloud-Top Temeperature and Cloud Growth Factor or Divergence Aloft Factor)^1 + Overshooting Top Factor^2 + Merger Factor^3 + Saturated Environment Factor^4] o Moisture Correction^5 Factor

END OF TECHNIQUE

cont. Fig, II. 4 Step 2 (factors 2, 3, 4 and 5) and step 3 of the convective storm technique.

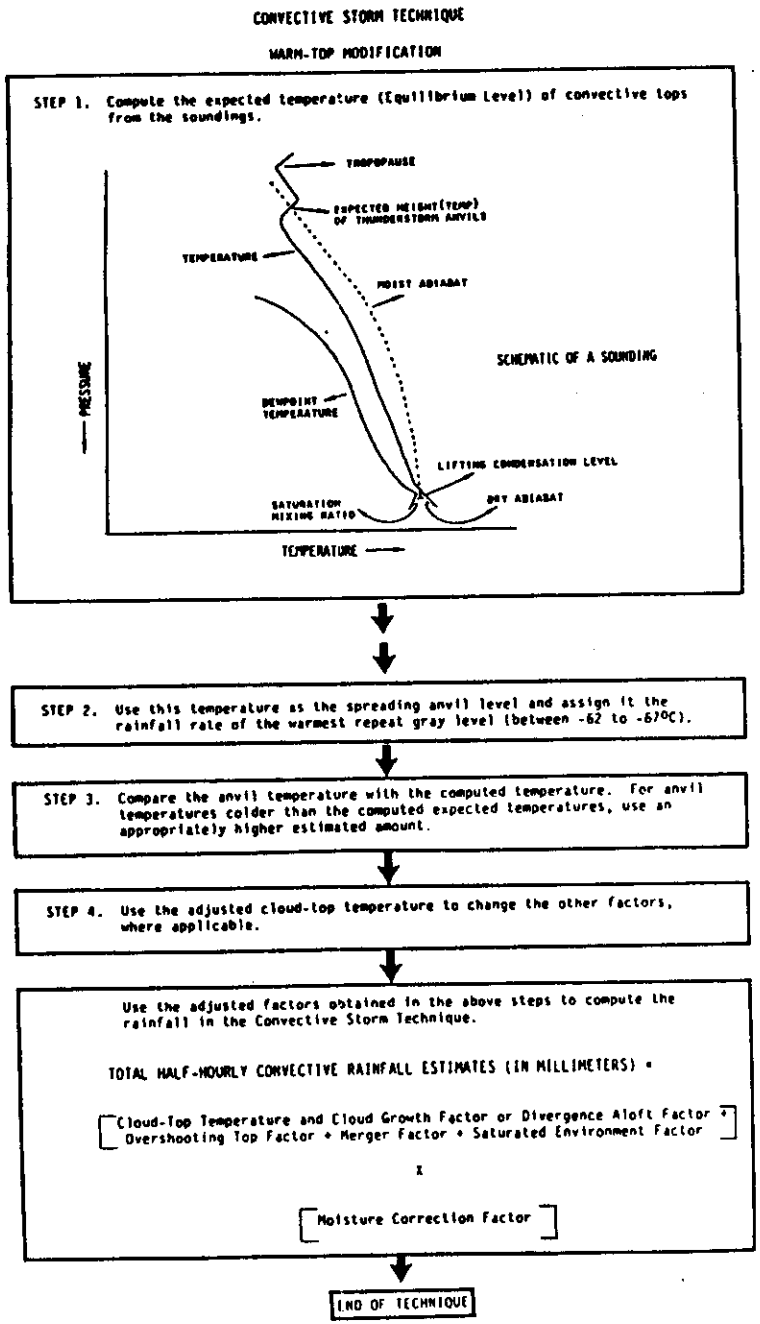

Fig. II.5 Convective storm technique warm-top modification.
(From Scofield, 1987)

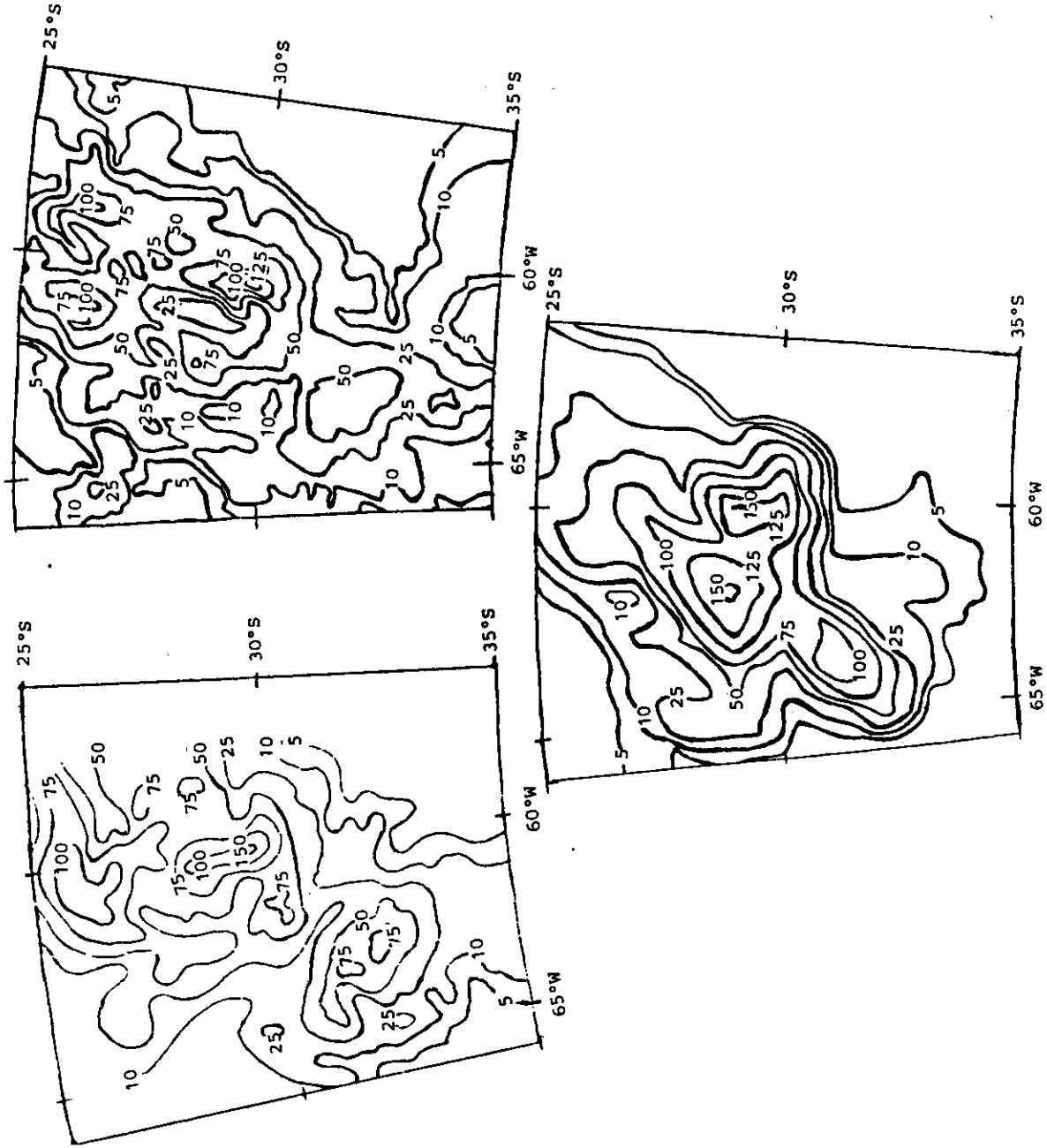


05:00 24JA83 17A-Z 0006-1640 FULL DISC IR